

# Transmitter-Side Channel Estimation in Magnetic Induction based Communication Systems

S. Kisseleff  
Institute for Digital Communications  
Friedrich-Alexander University  
Erlangen-Nürnberg, Germany  
Email: kisseleff@lnt.de

I. F. Akyildiz  
Broadband Wireless Networking Lab  
Georgia Institute of Technology  
Atlanta, USA  
Email: ian.akyildiz@ee.gatech.edu

W. Gerstacker  
Institute for Digital Communications  
Friedrich-Alexander University  
Erlangen-Nürnberg, Germany  
Email: gersta@lnt.de

**Abstract**—The use of magnetic induction (MI) based transmissions in challenging environments has been investigated in various works. Recently, a system model has been proposed, which explains how the pathloss of the magnetic induction based transmissions depends on the system parameters. It is frequently assumed, that perfect channel state information (CSI) is available at the transmitter and at the receiver, such that the optimal set of system parameters can be determined in order to maximize the overall data rate. However, in practical systems this knowledge may not always be easily acquired. In addition, a permanent feedback signaling is needed, in order to update the CSI at the transmitter. This feedback signaling usually occupies several time slots and therefore reduces the bandwidth efficiency. An interesting aspect, which has been overlooked in the past, is the channel estimation and prediction of the received signal within the MI transmitter circuit without explicit feedback signaling of CSI. In this paper, we investigate the potential of this technique for the wireless underground sensor networks.

## I. INTRODUCTION

Magnetic induction (MI) based communication systems are well known in the context of near-field transmissions (cf. [1]), energy harvesting and transfer (cf. [2]), and wireless sensor networks in challenging environments (cf. e.g. [3], [4]). In wireless underground sensor networks (WUSNs), the goal is to establish an efficient wireless communication in the underground medium. Typical applications for such networks include soil condition monitoring, earthquake prediction, border patrol, etc. [5]. Since the propagation medium is soil, rock, and sand, traditional wireless signal propagation techniques using electromagnetic (EM) waves can be only applied for very small transmission ranges due to a high pathloss and vulnerability to changes of soil properties such as moisture, [6]. MI-WUSNs make use of magnetic antennas implemented as coils, which are coupled via a quasi-static magnetic field. In previous work, some efforts were made to characterize the channel conditions of MI-based transmission, and its potential in different constellations and environments has been thoroughly investigated. In [7] and [8], sets of circuit parameters (resonance frequency and number of coil windings) have been proposed for maximizing the channel capacity of a single point-to-point transmission and for maximizing the network throughput of a tree-based WUSN, respectively. Modulation approaches for MI-based transmission are discussed in [9], which provides some insight into the MI-specific channel characteristics and corresponding optimized point-to-point transmission schemes.

Channel estimation is an essential signal processing block in

every communication system. Specifically, it enables a coherent channel equalization in the receiver and an optimum power control at the transmitter, which significantly improves the performance of a real system. However, in previous works on the magnetic induction based transmissions, this issue has been mostly overlooked. Perfect channel knowledge has been assumed in both transmitter and receiver, which is of course not realistic, especially when taking into account the harsh and possibly time-varying channel characteristics. Moreover, channel estimates can be used for triggering a frequency-switching procedure as described in [8]. Here, the goal is to detect and combat an abrupt change in the propagation conditions due to a sudden disaster and to notify the remaining sensor nodes to employ also a more advantageous transmission mode or even change the task assignment (e.g. switch between speech transmission and localization mode). Hence, the usability and efficiency of the system would increase, if such situations can be reliably detected.

A channel estimation at the receiver side can be established by utilizing the well-known approaches of blind or data supported estimation. Due to the stationary deployment of the system in the medium, the channel coherence time can be assumed very large in opposite to the traditional wireless and especially mobile communication scenarios. This is very beneficial for the estimation performance. Hence, nearly perfect estimation results can be assumed for the receiver. Therefore, in this paper we focus mostly on the transmitter-side channel estimation. We propose a technique, which is based on a unique property of the quasi-static magnetic fields, that effect at the same time transmitter and receiver. Thus, no explicit feedback signaling of the channel state information is needed in this approach. A closely related study on this issue can be found in [10]. Here, the main goal is a binary decision on the presence or absence of an eavesdropper, whose device interacts with the legitimate transceivers. When present, the eavesdropper coil causes changes of the channel transfer function by introducing additional power reflections within the resulting inductively coupled network. More precisely, the authors do not estimate the channel conditions, but only measure power reflections.<sup>1</sup> Hence, [10] does not provide details on the design of a channel estimation scheme for the MI based transmission channels, which is the main focus of our work.

<sup>1</sup>This is confirmed by the use of an energy detector in [10].

This paper is organized as follows. In Section II, the system model is presented, which comprises the basic system components for both transmitter and receiver and the channel characteristics. Based on these models, the feasibility of channel estimation at the transmitter is investigated in Section III. Section IV shows some numerical results and Section V finally concludes the paper.

## II. SYSTEM MODEL

In this work we utilize the channel and noise models proposed in [7], [8], and [9]. We assume that both transmitter and receiver devices contain the same set of passive circuit elements. Each circuit includes a magnetic antenna (which is assumed to be a multilayer air core coil) with inductivity  $L$ , a capacitor with capacitance  $C$ , a resistor  $R$  (which models the copper resistance of the coil), and a load resistor  $Z_L$ . The capacitor is designed to make the circuits resonant at the carrier frequency  $f_0 = \frac{1}{2\pi\sqrt{LC}}$ . The load resistor  $Z_L$  is chosen to minimize the power reflection at the receiver. These passive elements are selected according to [7]. The induced voltage is related to the coupling between the coils, which is determined by the mutual inductance  $M$  [11] given by [7]

$$M = \mu\pi N^2 \frac{a^4}{4r^3} (2\sin\theta_t \sin\theta_r + \cos\theta_t \cos\theta_r) \cdot G, \quad (1)$$

where  $r$  denotes the distance between the two coils,  $a$  stands for the coil radius,  $N$  is the number of windings, and  $\mu$  denotes the permeability of the medium.  $\theta_t$  and  $\theta_r$  are the angles between the coil radial directions of transmitter and receiver, respectively, and the line connecting the two coil centers [8]. Hence, the mutual inductance depends on the system parameters as well as the environmental parameters, which can vary over space and time. Specifically, the frequency selective attenuation  $G$  of the field strength in the medium (also known as eddy currents effect) implies time-varying frequency-selective changes of the transmission channel. However, due to transmission in a narrow band for the MI-based systems [3], the environmental changes (rainfalls, irrigation etc.) mostly do not effect the shape of the received signal spectrum, but solely its magnitude. Moreover, in order to be able to track the changes of the transmission channel properly, a maximum coherence time  $T_c$  needs to be taken into account.

As discussed in several previous works, see e.g. [7], the pathloss and channel capacity of the MI links heavily depend on the chosen system parameters, especially the resonance frequency  $f_0$  and the number of coil windings  $N$ . We assume an optimized system with a set of parameters that was proposed in [8]. Hence, we borrow the following equation for the optimum frequency  $f_0$  from this work:

$$f_0 = \left( \frac{2}{r\sqrt{\pi\sigma\mu}} \right)^2, \quad (2)$$

where  $\sigma$  denotes the conductivity of the medium. The number of coil windings  $N$  is set to the maximum value restricted only by the coil size.

In the following, we denote the current and voltage at the load impedance of the transmitter circuit as  $I_{Tx}$  and  $U_{Tx}$ , respectively. Correspondingly,  $I_{Rx}$  and  $U_{Rx}$  stand for the current and voltage at the load impedance of the receiver

circuit. The subscript  $TxRx$  indicates the direction of signal propagation from transmitter to receiver and  $TxTx$  stands for signal propagation from the signal source in the transmitter to the load impedance in the transmitter. The channel transfer function  $H_{TxRx}(f)$  can be calculated according to [9], taking into account the additional load impedance in the receiver [8]:

$$H_{TxRx}(f) = \frac{U_{Rx}}{U_{Tx}} = \frac{x_L}{(x + x_L)^2 - 1}, \quad (3)$$

where  $x_L = \frac{Z_L}{j2\pi fM}$  and  $x = \frac{R + j2\pi fL + \frac{1}{j2\pi fC}}{j2\pi fM}$ . Through this channel a sequence of quadrature amplitude modulated (QAM) symbols is transmitted. A smooth band-limited waveform with Fourier transform  $H_t(f)$  is used for pulse shaping. Thus, given the transmit filter  $A \cdot H_t(f)$  with the amplification coefficient  $A$ , the total consumed transmit power results from [7]

$$P_{\text{total}} = \frac{1}{2} \int_B \frac{|A \cdot H_t(f)|^2}{|j2\pi fM|} \frac{|x + x_L|}{|(x + x_L)^2 - 1|} df, \quad (4)$$

where  $B$  is the bandwidth of the transmitted waveform. Factor  $A$  can be determined to fulfill a given transmit power constraint. The receive noise power density spectrum is given by [7]

$$E\{P_N(f)\} \approx \frac{1}{2} \frac{4K_B T_K Z_L (R + Z_L)}{\left| R + j2\pi fL + \frac{1}{j2\pi fC} + Z_L \right|^2}, \quad (5)$$

where  $K_B \approx 1.38 \cdot 10^{-23}$  J/K is the Boltzmann constant,  $T_K = 290$  K is the temperature in Kelvin, and  $E\{\cdot\}$  denotes the expectation operator. Due to symmetry, this noise can be measured at the load impedances in both transceivers.

Because of the coupling between the coils, especially in environments with low-to-moderate pathloss, the changes in the transmission channel can effect the current flow in both circuits. In order to exploit this phenomenon for channel estimation, we first calculate the signal which arrives at the load impedance of the transmitter circuit during its own transmission. We start with a basic voltage equation for the transmitter circuit:

$$U_{Tx} = (R + j2\pi fL + \frac{1}{j2\pi fC} + Z_L) \cdot I_{Tx} - j2\pi fM \cdot I_{Rx}, \quad (6)$$

where  $I_{Rx} = I_{Tx} \cdot \frac{1}{x + x_L}$  cf. [7]. Using (6), we determine the transfer function from the signal source to the transmitter load impedance

$$H_{TxTx}(f) = \frac{x_L(x + x_L)}{(x + x_L)^2 - 1}. \quad (7)$$

Assuming that the receiver is deployed infinitely far away from the transmitter, an asymptotical result for the transfer function  $H_{TxTx}(f)$  can be obtained,

$$H_{TxTx,\infty}(f) = \frac{x_L}{x + x_L} = \frac{Z_L}{R + j2\pi fL + \frac{1}{j2\pi fC} + Z_L}, \quad (8)$$

which is independent of  $M$ . Hence, useful information about the channel conditions can be obtained by  $\Delta H_{TxTx}(f) = H_{TxTx}(f) - H_{TxTx,\infty}(f)$ , yielding

$$\begin{aligned} \Delta H_{TxTx}(f) &= \frac{x_L}{(x + x_L)^3 - (x + x_L)} \approx \frac{x_L}{(x + x_L)^3} \\ &= \frac{Z_L(j2\pi fM)^2}{(R + j2\pi fL + \frac{1}{j2\pi fC} + Z_L)^3} \end{aligned} \quad (9)$$

The transfer function  $H_{TxTx,\infty}(f)$  is easily acquired, since it only depends on the system parameters, which are known to both transceivers. The function  $\Delta H_{TxTx}(f)$  depends quadratically on the mutual inductance  $M$  as the only unknown parameter. Therefore, an estimate of the mutual inductance  $M$  and an estimate of  $H_{TxRx}(f)$  can be derived at the transmitter, which then can adjust its properties to the channel variations. Under the realistic assumption  $|x + x_L| \gg 1$  (where the well known issue of frequency-splitting in MI based channels is avoided) we can calculate the frequency-dependent signal-to-noise ratio (SNR) for  $TxTx$  and  $TxRx$  transmissions

$$\text{SNR}_{TxTx} = \frac{P(f) |\Delta H_{TxTx}(f)|^2}{E\{P_N(f)\}} \approx \frac{P(f)}{4K_B T_K} \frac{1}{|x + x_L|^4}, \quad (10)$$

$$\text{SNR}_{TxRx} = \frac{P(f) |H_{TxRx}(f)|^2}{E\{P_N(f)\}} \approx \frac{P(f)}{4K_B T_K} \frac{1}{|x + x_L|^2}, \quad (11)$$

where  $P(f)$  denotes the transmit power density at frequency  $f$ . Here,  $\frac{P(f)}{4K_B T_K}$  can be viewed as a transmit SNR of the equivalent communication system. The remaining parts,  $\frac{1}{|x + x_L|^4}$  and  $\frac{1}{|x + x_L|^2}$ , can be viewed as corresponding pathlosses  $L_{p,TxTx}$  and  $L_{p,TxRx}$ , respectively. Hence, the pathloss of the  $TxTx$  transmission is much larger than that of the  $TxRx$  transmission, which complies with our intuitive expectation.

We utilize the approach recently proposed for the direct MI uncoded signal transmissions [9]. Here, the total frequency band of the transmitted signal is subdivided in three sub-bands with unequal power distribution (optimized to achieve the highest possible data rate) and different bandwidths. With this approach, the difficulty of equalizing a very long impulse response of the MI based transmission channel is circumvented under moderate losses. The sub-band modulation scheme is then determined based on the signal-to-noise ratio at the output of the respective equalization filter for the considered sub-band. A root-raised cosine (RRC) waveform is used as signal pulse. For receive filtering we employ the whitened matched filter (WMF) [12]. Here, the overall discrete-time channel becomes minimum-phase, and the noise after sampling is white. Since the total transmission channel is frequency-selective, an equalization scheme is needed for the signal detection. In order to avoid further losses in data rate, for our performance investigations we use a decision-feedback equalization (DFE) scheme, which minimizes the mean-squared error (MSE) of the output signal (MMSE-DFE). For coded transmission, MMSE-DFE equalization would need to be replaced by Tomlinson-Harashima Precoding (THP) [13].

### III. CHANNEL ESTIMATION IN MI TRANSMITTER

Using the models introduced in Section II we propose algorithms for estimation of the absolute values of the mutual inductance. We assume knowledge about the initial value of  $M$ . This assumption is reasonable due to the network throughput based system optimization carried out in advance, like in [8], which is only possible if the initial environmental and system parameters are known to the system designer. Hence, the initial value of the mutual inductance is available at the transceivers. According to (10)-(11), the pathloss of the useful signal with respect to the load impedance of the transmitter is dramatically

higher than that with respect to the load impedance of the receiver. Therefore, it seems impossible to utilize the whole transmission band for estimation, since the SNR values in the transmitter at the band edges tend to reach values below  $-100$  dB. Hence, we focus on the middle band<sup>2</sup> for channel estimation in the transmitter. Furthermore, we exploit the knowledge of the transmitted symbols, which can be viewed as an uncorrelated training sequence of symbols which belong to a higher-order QAM constellation, cf. [9].

In order to obtain an appropriate signal for further processing, we subtract the transmitted signal filtered with (8) from the received signal at the load impedance of the transmitter. Hence, the resulting transmission channel is given by (9). The receive filtering can be done using the aforementioned WMF, which is now employed at the transmitter and matched to (9) and (5). Hence, we only need to consider the equivalent discrete-time signal model. Obviously, (9) is frequency-selective and corresponds to a very long impulse response in discrete time (more than 100 taps). For a successful channel estimation it is essential to determine all channel taps correctly, which yields a large set of variables to be estimated in a straightforward approach. On the contrary, if we exploit the information that the impulse response scales quadratically with the absolute value of the mutual inductance, the relation between modified and initial channel taps can be determined in advance, such that only one variable  $M$  needs to be estimated. Thus, the complexity of the estimation problem reduces and the precision increases. Therefore, the discrete-time signal at the input of the estimator needs to be equalized, such that only the impact of the scaling factor  $M^2$  remains. We model the absolute value of the modified mutual inductance  $M$  as  $M = \gamma M_0$ , where  $M_0$  denotes the initial value of the mutual inductance and  $\gamma$  is a positive real number. For an accurate estimation of  $M$  (and the channel impulse response) it is obviously enough to estimate  $\gamma$  and multiply it with the initial value  $M_0$ . For example, assuming that the system parameters are optimized for transmissions in dry soil, which becomes very wet according to [7], the mutual inductance decreases by a factor  $\gamma \approx 0.036$  (for any transmission distance).

The equalization is performed using an MMSE-DFE scheme.<sup>3</sup> In the following we utilize the discrete-time feedforward and feedback filters with transfer functions  $F_f(z)$  and  $F_b(z)$ , respectively, which have been optimized for this scheme [14]. Here, the traditional DFE equalization is modified, because the correct decisions at the output of the equalizer are the well-known training symbols. Thus, no real decision is needed and we avoid feeding back wrong decisions by replacing the signal at the input of  $F_b(z)$  by the training sequence. The bias correction [14] of the DFE filters is chosen to correct only the attenuation resulting from the initial impulse response. Additional attenuation/amplification may lead to a mismatch between  $F_f(z)$  and  $F_b(z)$ , which are adjusted to the initial

<sup>2</sup>As discussed in [9], the total transmission band is split up in three parts with two very steep transition zones. The sub-band in the middle has been shown to experience a much lower pathloss than the remaining side-bands.

<sup>3</sup>More advanced estimation techniques like maximum-likelihood sequence estimation (MLSE) are not applicable in this system due to a high modulation order and a very long impulse response of the discrete-time channel ( $\approx 100$  channel taps).

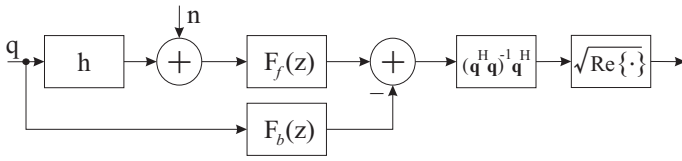


Fig. 1. Detection of changes in mutual inductance. Method 1.

impulse response. Of course, this imposes a higher intersymbol interference after equalization compared to the intersymbol interference after equalization for the initial channel. In order to cope with a very long impulse response (more than 100 taps) and very low SNR (below  $-30$  dB), we propose two methods for channel estimation. In the first method, the non-vanishing intersymbol interference is neglected due to an assumed much higher noise level. The estimation is based only on the equalized signal, which carries less energy in case of additional attenuation. The second method makes use of the intersymbol interference.

#### A. Method 1

We start from the discrete-time received signal  $y[k] = h[k] * q[k] + n[k]$  ( $*$ : convolution), where  $q[k]$  is a training sequence,  $h[k]$  stands for the discrete-time channel impulse response including the WMF, and  $n[k]$  represents additive white Gaussian noise. The resulting channel impulse response after the equalization can be assumed to have only one tap, where residual ISI is added to an equivalent total noise  $n_{\text{tot}}[k]$ . Thus, the equalized received signal  $z_{\text{eq}}[k]$  can be given by

$$z_{\text{eq}}[k] = h_{\text{eq}}[k_0] \cdot q[k - k_0] + n_{\text{tot}}[k], \quad (12)$$

with the equalized impulse response  $h_{\text{eq}}[k] = f_f[k] * h[k] - f_b[k]$ ,  $f_f[k] = \mathcal{Z}^{-1}\{F_f(z)\}$ ,  $f_b[k] = \mathcal{Z}^{-1}\{F_b(z)\}$  ( $\mathcal{Z}^{-1}\{\cdot\}$ : inverse z-transform), and a suitably chosen decision delay  $k_0$ . With a maximum-likelihood approach, an estimate  $\hat{h}_{\text{eq}}[k_0]$  of the reference tap of the equalized channel can be obtained via

$$\hat{h}_{\text{eq}}[k_0] = (\mathbf{q}^H \mathbf{q})^{-1} \mathbf{q}^H \mathbf{z}_{\text{eq}}, \quad (13)$$

where  $\mathbf{q}$  and  $\mathbf{z}_{\text{eq}}$  are column vectors of same length and contain the complex symbols of sequence  $q[k - k_0]$  and  $z_{\text{eq}}[k]$ , respectively. The expectation value of the reference tap of the equalized channel equals  $\gamma^2$ . Therefore, in order to determine an estimate of  $\gamma$ , a square-root operation is applied to the real part of  $\hat{h}_{\text{eq}}[k_0]$ . The entire signal processing scheme for the transmitter is depicted in Fig. 1. Due to an extremely low SNR of the input signal, a very long training sequence is needed for a reliable computation. We assume a continuous transmission, such that enough transmitted symbols can be used for the estimation. However, we have to restrict the length of the sequence  $L_s$  per burst by taking into account the coherence time  $T_c$  and the bandwidth  $B_{\text{mid}}$  of the mid sub-band:

$$L_s \leq T_c \cdot B_{\text{mid}}. \quad (14)$$

The coherence time is assumed to be very long in soil, because the properties of a dense medium are usually slowly time-varying or even frequently assumed to be constant over time. Due to a lower pathloss for transmissions in free space, the

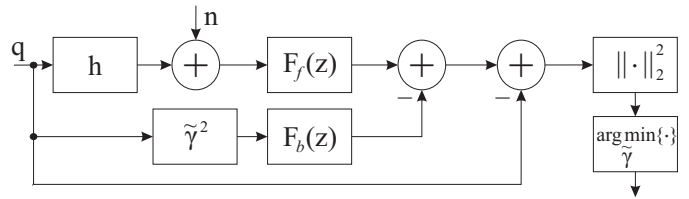


Fig. 2. Detection of changes in mutual inductance. Method 2.

SNR for channel estimation is dramatically higher, such that a coherence time of one second is already enough for obtaining a reasonable estimation accuracy.

#### B. Method 2

As discussed previously, due to a mismatch of  $F_f(z)$  and  $F_b(z)$  of the DFE scheme for the modified channel, the intersymbol interference has an additional impact on the distortion power for channel estimation. Obviously, the interference is minimum only when  $F_f(z)$  and  $F_b(z)$  are matched properly to the channel. Hence, the estimation problem can be viewed as finding the optimal scaling for the filter  $F_b(z)$ , such that the mean-squared error (MSE) at the output of the DFE is minimized:

$$\hat{\gamma} = \arg \min_{\tilde{\gamma}} \|z_{\text{eq}}(\tilde{\gamma}) - \mathbf{q}\|_2^2, \quad (15)$$

where  $\|\cdot\|_2^2$  denotes the L<sub>2</sub>-norm applied to a vector and  $z_{\text{eq}}(\tilde{\gamma})$  indicates that the equalization depends on the scaling of the feedback filter. The resulting signal processing is shown in Fig. 2. Here,  $\tilde{\gamma}$  is a possible candidate for the estimate of  $\gamma$ . After the filtering, the MSE for each candidate is calculated and the candidate  $\hat{\gamma}$  with the lowest MSE is picked as the most likely estimate of  $\gamma$ . This approach is similar to the minimum output energy detector from [15] applied to  $z_{\text{eq}}$ .

## IV. NUMERICAL RESULTS

In this section, we discuss numerical results on the performance of the proposed channel estimation methods. In our simulations, we assume a total transmit power of  $P_t = 10$  mW. We utilize coils with wire radius 0.5 mm and coil radius  $a = 0.15$  m. The maximal number of coil windings  $N$  is 1000. The conductivity and permittivity of dry soil are  $\sigma = 0.01$  S/m and  $\epsilon = 7\epsilon_0$ , where  $\epsilon_0 \approx 8.854 \cdot 10^{-12}$  F/m. Since the permeability of soil is close to that of air, we use  $\mu = \mu_0$  with the magnetic constant  $\mu_0 = 4\pi \cdot 10^{-7}$  H/m. For a reduced pathloss,  $\theta_t = \theta_r = \pi/2$  is assumed. The target symbol error rate is selected to  $\text{SER}_t = 1.5 \cdot 10^{-3}$ , and the roll-off factor of the used RRC transmit filter is 0.25.

For the evaluation of the proposed channel estimation methods, we assume that perfect Channel State Information (CSI) is available at the receiver. After every estimation of  $\gamma$ , the transmit power is increased if necessary in order to compensate an unforeseen attenuation. Due to a limited power budget in small sensor devices, we provide results for a maximum transmit power  $P_{t,\text{max}} = 100$  mW, which corresponds to at most 10 dB power increase with regard to the initial transmit power of 10 mW. Therefore, the smallest  $\gamma$ , which can be compensated in the transmitter is  $\gamma_{\text{min}} = \sqrt{\frac{1}{10}}$ . For  $\gamma < \gamma_{\text{min}}$ , the maximum transmit power  $P_{t,\text{max}}$  is not enough to compensate the attenuation and we observe a performance degradation.

Our performance measure is the mean-squared error (MSE) for the estimated value of  $\gamma$  and the symbol error rate (SER) observed at the receiver in the mid sub-band. The CSI is assumed to be perfectly known in the receiver due to the reasons provided in Section I. We perform 1000 channel estimations for each value of  $\gamma$ . For  $\gamma > 1$ , the estimation becomes more and more reliable, yielding  $SER \approx SER_t$ . Therefore, we focus on more crucial channel conditions for  $\gamma \in [0, 1]$ . Based on the estimates, the attenuation of the  $TxRx$  transmission channel is compensated by scaling the transmit signal with  $\frac{1}{\gamma}$ . Through the compensated channel, 2000 symbols are transmitted. In total,  $2 \cdot 10^6$  symbols are received and SER is obtained. Due to a higher-order modulation in the mid sub-band, the highest possible SER can be larger than 0.5.

In the following three channel constellations are investigated in order to visualize the system behavior for different transmission distances and different environments. In dry soil, the channel estimation is shown for distances of 25 m and 35 m, respectively. For transmissions in free space, the results are presented only for 25 m initial distance in order to compare it with the corresponding results in soil. For transmissions in dry soil, we assume a coherence time of  $T_c \in [5, 10]$  min. for 25 m and  $T_c \in [10, 20]$  min. for 35 m, respectively. For transmissions in free space,  $T_c = 1$  sec is assumed.

In Figs. 3, 4, and 5, the mean-squared errors of the estimation of  $\gamma$  are shown. We observe that method 2 performs almost equally well as method 1 in dry soil at short transmission distance (see Fig. 3) or even significantly better at longer distances (see Fig. 4), because the first method needs a high SNR for a reliable estimation of the signal attenuation. On the contrary, for the second method, the signal-to-intersymbol interference ratio (SIR) is more important. Therefore, for weak channels (e.g. in medium or at longer transmission distances) method 2 outperforms method 1. However, the estimation results for such channels are not very useful,  $MSE \geq 0.3$  for 35 m distance in dry soil. Due to the same reason, method 1 outperforms method 2 in free space with 25 m distance. Here, we observe a much lower estimation error, which is due to a lower pathloss.

In Figs. 6, 7, and 8, the symbol error rates for different values of  $\gamma$  are shown. These error rates correspond to the scenarios considered in Figs. 3, 4, and 5, respectively. Of course, with larger values of  $\gamma$ , a very low SER can be reached. However, error rates below  $SER_t$  are not demanded and we can save transmit power in these cases. Obviously, without any channel estimation in the transmitter, the resulting SER becomes unsatisfactory even with relatively large  $\gamma$ , e.g.  $\gamma = 0.8$  or  $\gamma = 0.6$ . Due to a quite small MSE of the estimated  $\gamma$  for short transmission distances, much lower SER can be reached than without estimation (see Figs. 6 and 8). An important observation is that even with a substantially larger MSE of method 2 compared to method 1 in free space, the resulting SER is only slightly better. Moreover, for larger transmission distances (see Fig. 7), a very high pathloss leads to a degradation of the performance for method 1. Obviously, for larger values of  $\gamma$ , channel estimation based on method 1 is even less efficient than no channel estimation, whereas using method 2 the resulting SER is at least two times less than without estimation.

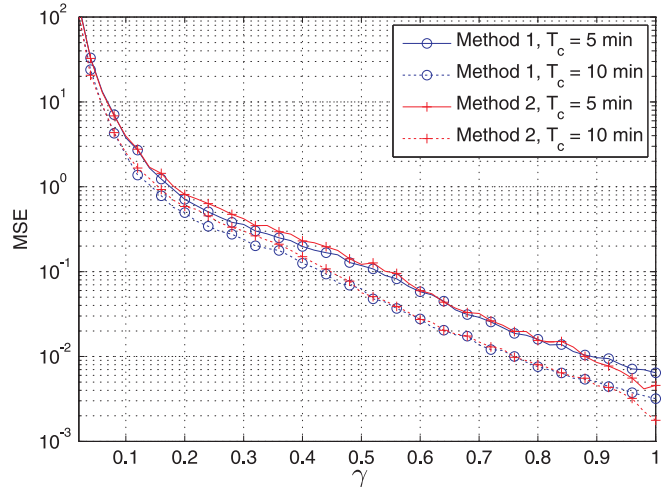


Fig. 3. Mean-squared error of  $\gamma$  estimation for 25 m distance in dry soil.

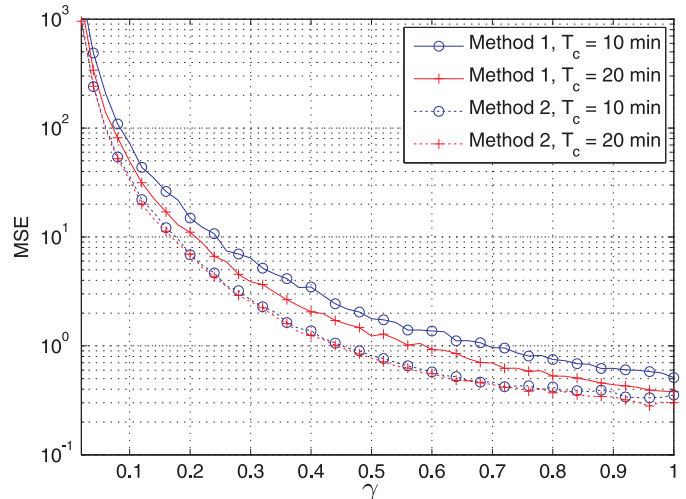


Fig. 4. Mean-squared error of  $\gamma$  estimation for 35 m distance in dry soil.

In general, benefits of channel estimation in the transmitter can be observed compared to the system without estimation. Although a large MSE occurs for badly conditioned channels (i.e., high pathloss), the resulting error rates can be further reduced by applying e.g. adaptive channel coding. However, this enhancement remains open for future investigations.

## V. CONCLUSION

In this paper we have considered channel estimation at an MI transmitter without explicit feedback signaling of the channel state information from the receiver. This technique is based on fundamental properties of the MI-based transmission channels, which effect the current flow in the connected transceivers and therefore enable a direct estimation of the received signal attenuation in the transmitter. We proposed two methods which exploit this phenomenon. The first approach is based on noise suppression by collecting a vast amount of signal samples within a long coherence time interval and performing some averaging. The second approach makes use of the mismatch between the feedforward and feedback equalization filters of DFE, which introduces an additional intersymbol interference based on the channel attenuation. In addition, we took into account the maximum available transmit power, which restricts

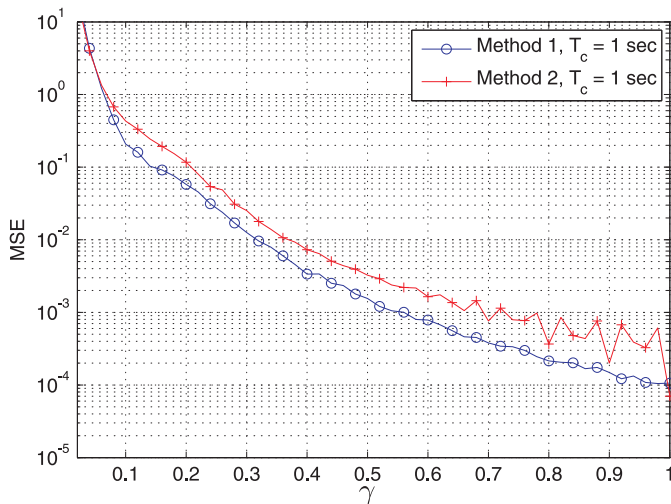


Fig. 5. Mean-squared error of  $\gamma$  estimation for 25 m distance in free space.

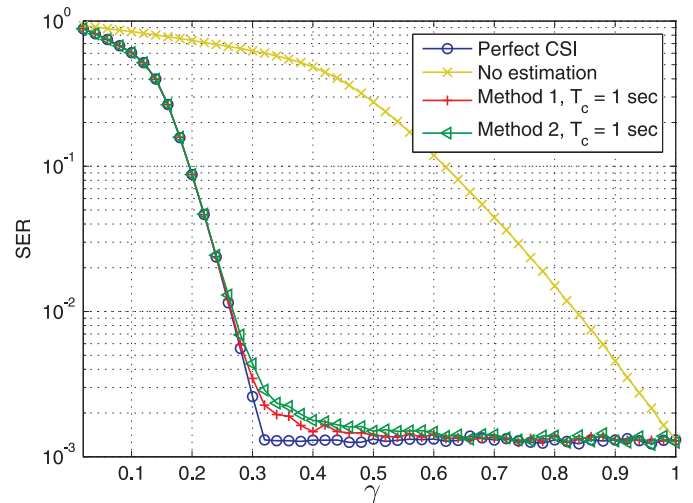


Fig. 8. Symbol error rate in the mid sub-band at the receiver for 25 m distance in free space.

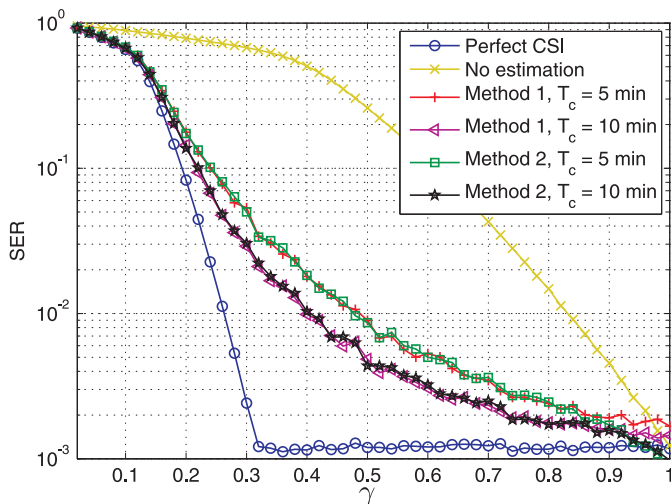


Fig. 6. Symbol error rate in the mid sub-band at the receiver for 25 m distance in dry soil.

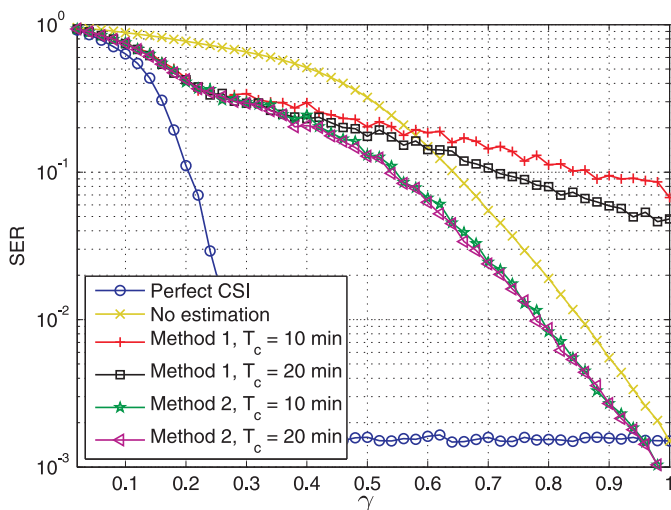


Fig. 7. Symbol error rate in the mid sub-band at the receiver for 35 m distance in dry soil.

the compensation of the pathloss. For the simulated scenarios, the mean-squared errors of the estimated channel attenuation and the symbol error rate at the receiver have been presented. The two proposed methods have been compared and their benefits and drawbacks discussed.

#### REFERENCES

- [1] R. Bansal, "Near-field magnetic communication," in *IEEE Antennas and Propagation Magazine*, April 2004.
- [2] A. Karalis, J.D. Joannopoulos, and M. Soljacic, "Efficient wireless non-radiative mid-range energy transfer," *Annals of Physics*, vol. 323, pp. 34–48, January 2008.
- [3] Z. Sun and I.F. Akyildiz, "Magnetic induction communications for wireless underground sensor networks," *IEEE Trans. on Antennas and Propag.*, vol. 58, pp. 2426–2435, July 2010.
- [4] M.C. Domingo, "Magnetic Induction for Underwater Wireless Communication Networks," *IEEE Trans. on Antennas and Propag.*, pp. 2929–2939, April 2012.
- [5] I.F. Akyildiz, W. Su, Y. Sankarasubramaniam, and E. Cayirci, "Wireless sensor networks: A survey," *Comput. Netw. J.*, vol. 38, pp. 393–422, March 2002.
- [6] L. Li, M.C. Vuran, and I.F. Akyildiz, "Characteristics of underground channel for wireless underground sensor networks," in *Proc. IFIP Mediterranean Ad Hoc Networking Workshop 2007*, June 2007.
- [7] S. Kisseleff, W.H. Gerstacker, R. Schober, Z. Sun, and I.F. Akyildiz, "Channel capacity of magnetic induction based wireless underground sensor networks under practical constraints," in *Proc. of IEEE WCNC 2013*, April 2013.
- [8] S. Kisseleff, I.F. Akyildiz, and W. Gerstacker, "Interference Polarization in Magnetic Induction based Wireless Underground Sensor Networks," in *Proc. of IEEE PIMRC 2013 (SENSA Workshop)*, September 2013.
- [9] —, "On Modulation for Magnetic Induction based Transmission in Wireless Underground Sensor Networks," *accepted for publication at ICC 2014*, 2014.
- [10] L.R. Varshney, P. Grover, and A. Sahai, "Securing inductively-coupled communication," in *Information Theory and Applications Workshop (ITA) 2012*, February 2012.
- [11] Z. Sun and I.F. Akyildiz, "On capacity of magnetic induction-based wireless underground sensor networks," in *Proc. of IEEE INFOCOM 2012*, March 2012, pp. 370–378.
- [12] J.G. Proakis, *Digital Communications*. McGraw-Hill Higher Education, 2001.
- [13] G.D. Forney and G. Ungerboeck, "Modulation and Coding for Linear Gaussian Channels," *IEEE Trans. on Information Theory*, vol. 44, no. 6, pp. 2384–2415, October 1998.
- [14] J.M. Cioffi, G.P. Dudevoir, M.V. Eyuboglu, and G.D. Forney, "MMSE Decision-Feedback Equalizers and Coding," *IEEE Trans. on Communications*, vol. 43, pp. 2582–2594, October 1995.
- [15] M. Honig, U. Madhow, and S. Verdú, "Blind adaptive multiuser detection," *IEEE Trans. on Information Theory*, pp. 944–960, July 1995.